Received: 28 March 2020 | Revised: 1 November 2020 | Accepted: 16 November 2020

IET Electric Power Applications

DOI: 10.1049/elp2.12030

The Institution of Engineering and Technology WILEY

ORIGINAL RESEARCH PAPER

An axial passive magnetic bearing using three PM rings

Fabrizio Marignetti[1] | **Milad AlizadehTir**[1] | **Seyyed Mehdi Mirimani**[2]

[1]Department of Electrical and Information Engineering, University of Cassino and South Lazio, Cassino, Italy

[2]Faculty of Electrical and Computer Engineering, Babol Noshirvani University, Babol, Iran

Correspondence

Fabrizio Marignetti, Department of Electrical and Information Engineering, University of Cassino and South Lazio, Cassino, 03043 Italy.
Email: marignetti@unicas.it

Funding information

Regione Lazio, Grant: L.R. 13/200 art.4

Abstract

The results of numerical and experimental analysis of passive magnetic bearings are presented. The proposed structure is composed of three radially stacked ring-shaped permanent magnets. The improvements of stiffness and load capacity are proven in comparison to the classical passive magnetic bearing composed of two rings. A preliminary sensitivity analysis is carried out by means of the 2-dimensional finite element method (FEM) modelling, which is used to provide the initial points for the stochastic optimisation and also to define the best fitness and penalty functions. Finally, the 2-dimensional FEM is used to compare the force density and the cost of the proposed structure to those of the classical passive magnetic bearing composed of two rings. The optimised structure was manufactured and validated by experimental measurements. The proposed passive magnetic bearing exerts greater axial force and stiffness than similar structures.

1 | INTRODUCTION

Economical reasons and energy savings are key issues in industries, especially for those using rotational systems [1,2]. The introduction of magnetic suspension systems using permanent magnets (PMs) helped solving industrial problems in special operating conditions such as aerospace, flywheels and turbomolecular pumps, radiation, vacuum and clean room environments, and equipment for severe conditions, for example, low temperature and rotational speeds over 10,000 rpm [3–9].

In fact, magnetic suspension introduces significant technical advantages [10], such as no wearing and long life span, extreme reliability, friction less and lubrication free operation, low losses, low maintenance cost, low acoustic noise, zero resistance in comparison to conventional mechanical ball bearings [3–8,10–16].

Magnetic levitation was introduced in 1842 as a consequence of Earnshaw's theorem [17]. In the mid-1930s, Beams and Holms built the first practical magnetic bearing, which falls into the passive magnetic bearing (PMB) category [13].

Magnetic bearings can be classified according to Lorentz force and reluctance force. This classification includes eight types of magnetic bearings in which three mentioned types of bearings are presented and divided into some subset types [18].

Another classification method is based on the principle of production of magnetic forces in magnetic bearings and the regulation of their operation. According to this classification, magnetic bearings are classified into three types: PMB, active magnetic bearing (AMB) and hybrid magnetic bearing (HMB) [5,19].

According to the degree of freedom, the rotational PMBs can be divided into axial and radial PMBs.

An axial PMB composed of three ring-shaped PMs is experimented in order to prove the improvement of the magnetic force and stiffness. The proposed structure has outer and inner rings that are connected together and to the stator, while the middle ring is connected to the rotor. The proposed structure is more complex than the classical PMB composed of two rings; therefore its advantages are assessed in terms of its force density. The magnetic force is computed, and a comparison is performed between the proposed structure and an equivalent PMB with two magnets.

The purpose of this study is threefold:

1. introducing a new structure of passive magnetic bearing composed of three independent rings. The novelty of the structure is discussed in Section 2;
2. providing a stochastic optimisation method;
3. comparing the proposed bearing to the classical magnetic bearing.

The finite element method (FEM) is used for the magnetic force calculation. The PMBs are modelled using

two-dimensional FEM (2D-FEM), exploiting the axial symmetry around *z*-axis. The comparison of the proposed structure of PMB to an equivalent structure with two magnets and optimised dimensions is finally carried out. To optimise the dimensions of both PMB structures, the genetic algorithm (GA) is used. As a basic principle, GA needs some initial points and fitness and penalty functions in order to provide convergence towards the objective function; therefore, sensitivity analysis is applied to investigate the bearing characteristics.

The results of the sensitivity analysis produced by FEM have been saved in a database to generate a black box defining the PMB characteristics. During the GA process, the data needed by the GA is recalled from the database. If the recalled data is not included in the database, the result is produced by linear interpolation from the data stored in the database.

The force density is used as an index in order to investigative the effectiveness of the proposed bearing. In fact, the volume of the magnetic material is one of the most important pieces of the expenses puzzle. Therefore, both the force and the force density are considered to compare the two PMB structures. Finally, the optimised three-ring PMB was manufactured, and a special setup was built. The experiments show an agreement between the 2D-FEM results and the practical tests. The structure of the study is as follows: Section 2 provides the basic model of the bearing and the motivations behind this work, Section 3 provides details on the construction of the bearing, Section 4 shows the FEM analysis, while the sensitivity analysis, which is used to build the initial database, is explained in Section 5. The GA and the consequent optimisation are explained in Section 6. The results are discussed in Sections 7 and 8.

2 | MAGNETIC FORCE AND STIFFNESS

The simplest structure of PMB is shown in Figure 1a. This traditional PMB comes in two versions: the first consists of two concentric rings separated by a cylindrical air gap, and the second includes two rings of the same dimension separated by a planar air-gap. Hereafter, the first version is considered. Also, Figure 1b shows the new PMB structure with the mesh, which is used in Section 4. The PMB is characterised by the interaction force (F) between the magnets and the derivative of the force, namely the stiffness (K). In the Cartesian coordinate reference system, the static loading capacity and the stiffness are given by:

$$\vec{F} = F_x\vec{x} + F_y\vec{y} + F_z\vec{z} \tag{1}$$

$$\vec{K} = -\left(\frac{\mathrm{dF_x}}{\mathrm{d}x}\vec{x} + \frac{\mathrm{dF_y}}{\mathrm{d}y}\vec{y} + \frac{\mathrm{dF_z}}{\mathrm{d}z}\vec{z}\right) \tag{2}$$

$$\vec{K} = -(K_x\vec{x} + K_y\vec{y} + K_z\vec{z}) \tag{3}$$

According to Earnshaw's theorem [14], the sum of the bearings' stiffnesses in the three dimensions must be equal to zero, that is:

$$K_x + K_y + K_z = 0 \tag{4}$$

Exploiting the circular shape of the rings one has: $K_x = K_y = K_r$; in the cylindrical coordinates:

$$K_z = -\ 2K_r \tag{5}$$

Therefore, the ratio between axial and radial stiffnesses is always - 2 for pure PM configurations with rotational symmetry [20].

If K_z is known, then the stiffness of the bearing is determined. The stiffness needs be positive to achieve a stable configuration, although Equation (4) indicates that a positive value of K_r results into a negative value of K_z [21] and vice versa, so there is a very strong coupling between axial and radial stiffnesses of cylindrical radial magnetic bearings. The radial PMB, which is designed to hold radial loads, is unstable in the axial direction, so to ensure stability along the rotation axis, other means are required (e.g. one thrust bearing or an electromagnetic action). In this paper, the magnetic interaction between the magnets is used to generate an axial force.

There are several ways to calculate the magnetic force between PMs. In [22], a 2-D semi-analytical method is used for the magnetic force calculation. In [23], the force calculation is done using special functions. In [21], a semi-analytical method is used in cooperation with the Coulombian model to achieve the magnetic forces, and it is shown that both the air-gap and the PM width have a strong influence on the magnetic force. In this study, the Finite Element Analysis (FEA) is used in order to calculate the magnetic force.

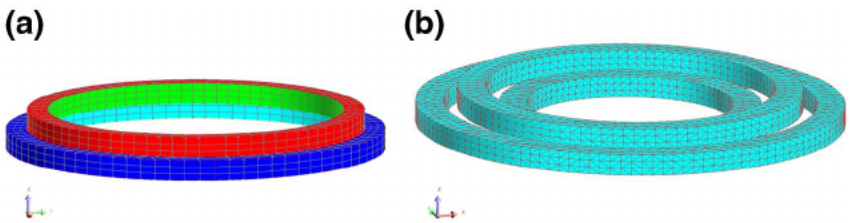

FIGURE 1 Three-dimensional model of PMB: (a) using two PM bearings and (b) proposed structure and its mesh diagram

3 | THE NEW STRUCTURE OF PMB

Figure 2a shows the common structure of PMB with two PM rings installed in a motor. The outer magnet is connected to the stator while the inner ring rotates with the rotor. In this structure, the axial displacement is the displacement of the inner ring from the centred (neutral) point.

The proposed structure consists of three PM rings, as shown in Figure 2b. Both the outer and the inner rings are coupled to the stator using two mechanical holders, while the middle ring is connected to the rotor. An axial displacement happens when the middle ring moves from the aligned (neutral) position, together with the rotor.

Although the scientific literature provides many examples of axially and radially stacked PMB, [24–27], the traditional stacked PMBs are built by axially or radially gluing a number of rings to form two rigid structures, fixed to the stator and to the rotor, respectively. The two structures are composed of the same number of magnets and are separated by one airgap. The increase of the force and of the stiffness provided by this kind of bearings is already known. In fact, stacking is considered an effective method to increase the force, as it allows multiplying the force provided by each elementary unit while reducing the parts where the field interaction is less effective. In the proposed bearing, instead, the number of rings of the two elements is different, and the rotating and the fixed rings are interleaved (not just opposed); there are two airgaps, and there is no elementary unit, which repeats itself. The field distribution is therefore different from the traditional stacked bearing, and the whole structure needs be optimised.

An extra volume of magnets achieves higher force. In order to perform a fair comparison, the traditional and the new structure should be compared in the same condition, that is. considering the same magnetic force.

The proposed geometry structure is shown in Figure 3, where J is the magnetic polarisation vector. Also three PM rings are radially centered and axially magnetised. The main geometric parameters are in Table 1. The results of sensitivity analysis performed with FEM will passed on GA as the starting points for optimisation.

4 | FINITE ELEMENT SIMULATION

The semi-analytical methods, proposed by Ravaud et al. [28,29] to investigate force and stiffness in PMB with both axial and radial magnetisation, are complex. They use elliptic integrals and neglect the leakage fluxes. Conversely, FEM allow a precise analysis of magnetic field taking into account all geometry details and non-linearities.

In order to model the new structure, we suppose that the external and the internal rings have fixed positions, and all magnets are made with the same material, that is Neodymium–Iron–Boron (NdFeB). The temperature coefficient of the magnets is 1.6×10^{-3} T/ C. The operating temperature is 53 C. A 2D axisymmetric study of the novel structure can be carried out due to the axial symmetry around z-axis. The geometric representation of the device is presented over a cross section plane as shown in Figure 4, where also the mesh diagram is shown. The mesh has about 18,000 elements and 35,000 nodes. Increasing the number of elements does not provide significant changes to the solution. The isovalue model of the tested structure for the conventional and proposed structures of PMB is shown in Figures 5a and 6a, respectively.

5 | SENSITIVITY ANALYSIS AND INITIAL DATA GATHERING

PM rings can be radially or axially magnetised. As radial magnetisation is complex and expensive, axially magnetised magnets have been considered in this investigation as it is shown for the PMB using two PMs and for the proposed PMB in Figures 5b and 6b, respectively.

A simple comparison is shown in Figure 7, considering the dimensions in Table 2, between the results of the FEM

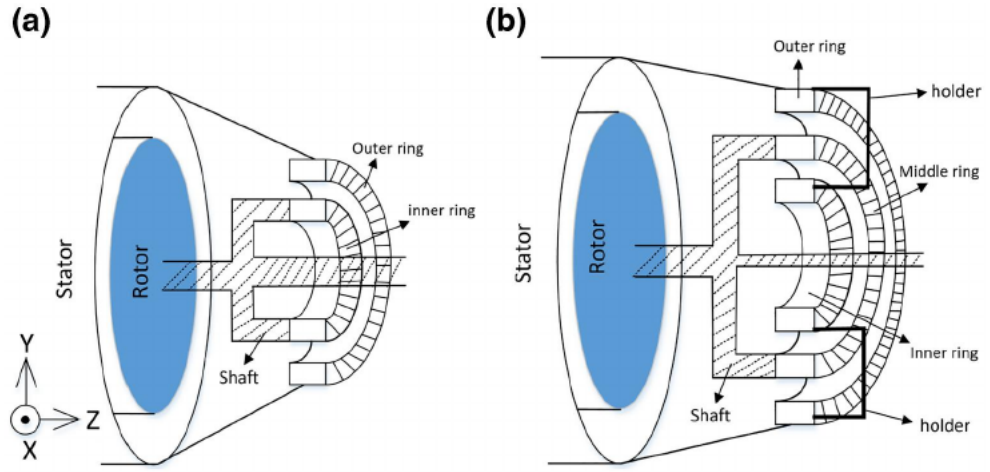

FIGURE 2 Schematic representation of the classical PMB.: (a) prevalent structure and (b) proposed structure

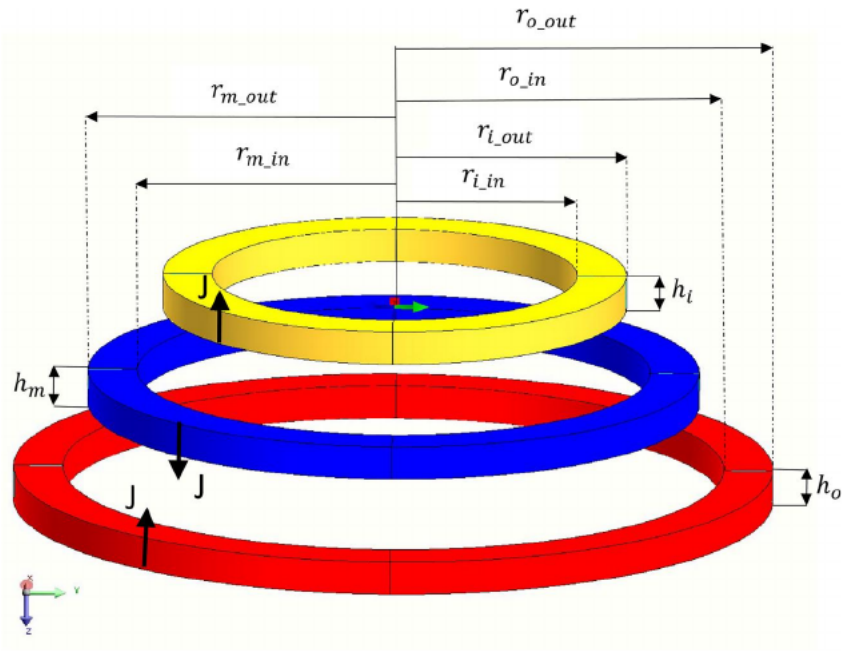

FIGURE 3 Representation of the new structure of passive magnetic bearing (PMB) with three-ring permanent magnet (PM) with nomenclature

TABLE 1 Initial dimensions of the proposed PMB

Symbol	Quantity	Value (mm)
r_{o_out}	Outer radius of the outer ring	28
r_{o_in}	Inner radius of the outer ring	25
r_{m_out}	Outer radius of the middle ring	24.9
r_{m_in}	Inner radius of the middle ring	21.9
r_{i_out}	Outer radius of the inner ring	21.8
r_{i_in}	Inner radius of the inner ring	18.8
h_o	Outer ring height	3
h_m	Middle ring height	3
h_i	Inner ring height	3

Abbreviation: PMB, passive magnetic bearing.

simulation and the semi-analytical approach for validation FEA result [28]. The maximum amplitude is 67 N, and the results of the two methods are very close together. As it seen, the maximum force amplitude of the proposed structure, whose dimensions are given in Table 1, is 120 N while the proposed PMB is non-optimised. Figure 8 shows that the maximum stiffness is increased in the proposed structure compared to the PMB with two PMs. The maximum stiffnesses are 182.141 and 32.50 N/mm, respectively.

5.1 | Influence of the air gap dimensions

To investigate the effects of each parameter on the PMB performance, one parameter at a time is varied, while keeping the other dimensions of the rings. To evaluate the influence of the air-gaps thickness, both air-gap length are changed together. Figure 9 shows the effects of the air-gap width on the magnetic force versus the axial displacement of the middle ring. The dimensions of the PMB considered in this stage of the sensitivity analysis are in Table 3. According to Figure 9, the smaller the air-gap width, the larger the axial force. The minimum possible air-gap width should be selected considering mechanical restrictions, to avoid wearing in the practical structure, so the air-gap width is chosen as 0.2 mm.

According to Equation (2), the axial stiffness graph can be achieved by derivation of the force diagram. The stiffness graph is shown in Figure 10. It can be concluded that the maximum amplitude of the stiffness is achieved when the air-gap width is smaller and also when the force amplitude is zero; it means that the maximum slope of the force diagram is located at the zero position.

5.2 | Influence of the height

The sensitivity analysis of the middle-ring height is done according to the dimensions in Table 4. The height of the outer and of the inner rings are constant and are selected the same as each other equal to 3 mm as an assumption. Figure 11 (a) shows the axial force versus the axial displacement of the middle ring for different middle ring height. The force amplitude reaches its maximum value when the middle ring height is equal or higher than the value of inner and outer rings' heights, which are the same as each other. However, the force amplitude maximisation is only one of the objectives, like the volume of used magnets as the economic factor should be also considered for the selection the best height.

The maximum amplitude of the axial force together with the force density versus different middle ring heights is presented in Figure 11b. The maximum axial force for the middle

FIGURE 4 Two-dimensional mesh model

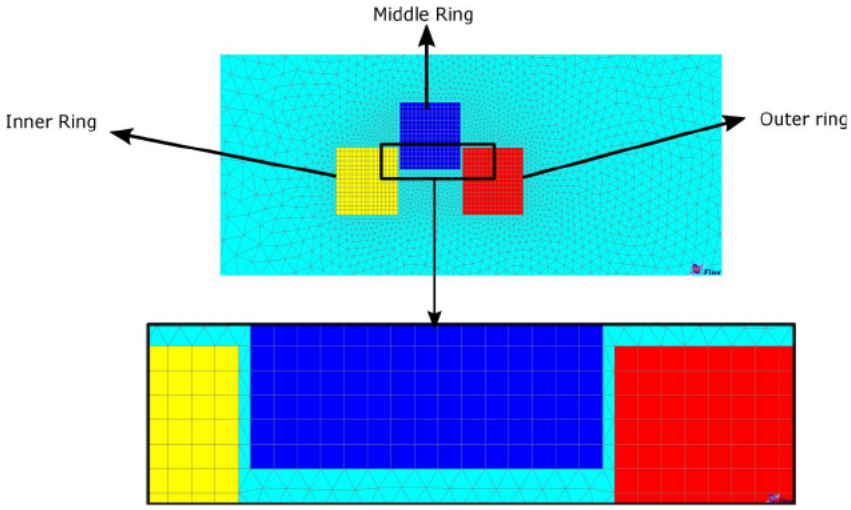

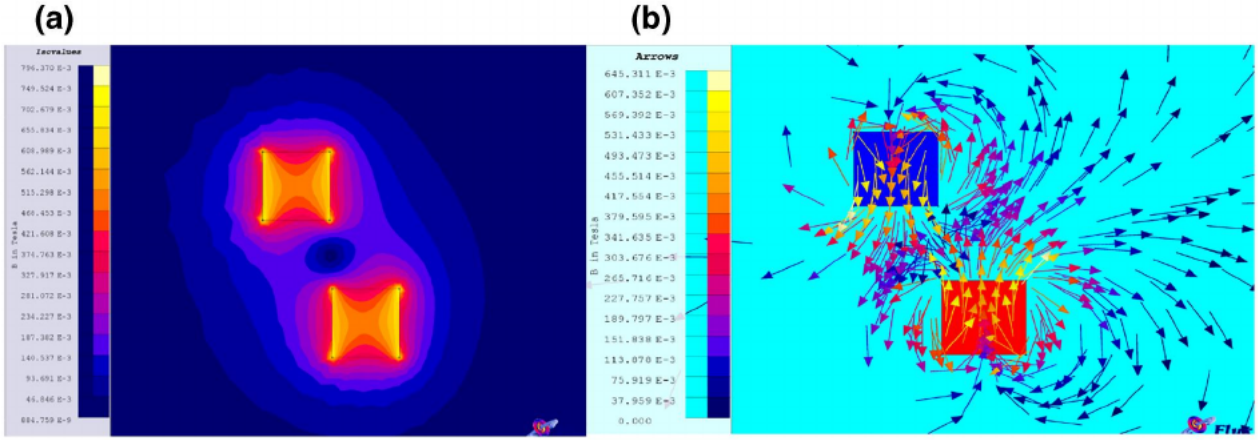

FIGURE 5 Representation of the magnetic properties of the passive magnetic bearing (PMB) with two permanent magnets (PMs): (a) flux density and (b) magnetisation direction

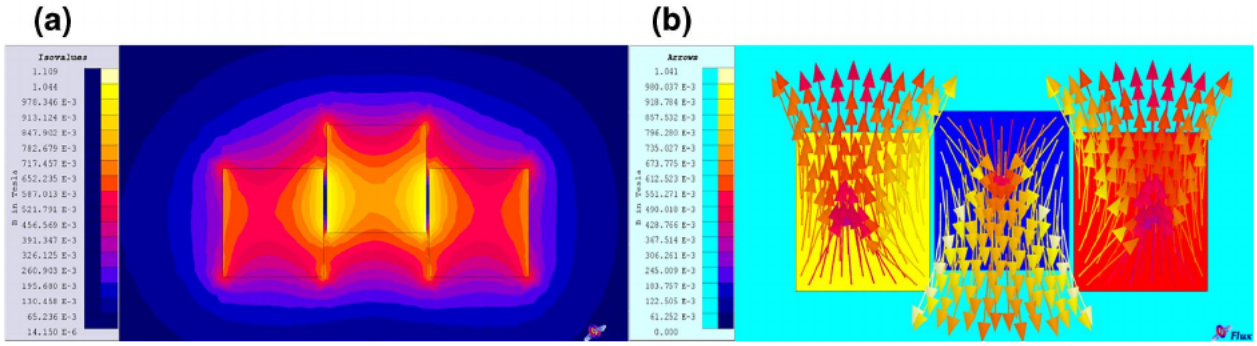

FIGURE 6 Representation of the magnetic properties of the proposed passive magnetic bearing (PMB): (a) flux density, (b) magnetisation direction

ring with the heights of 3 and 5 mm is, respectively, 134.73 and 145.59 N. The difference between them is 10.86 N which means 7.46%, that is, less than 10%. Increasing the height over this values does not produce a stronger force and just increases the costs. Force density can be chosen as a good reference for the comparison of the two structures:

$$Force\ density = \frac{maximum\ amplitude\ of\ the\ force}{volume\ of\ the\ magnets} \quad (6)$$

A trade off must be applied between the maximum force amplitude and the force density. As it is seen, the force density is stronger if the middle ring height is 3 mm; so, this height can

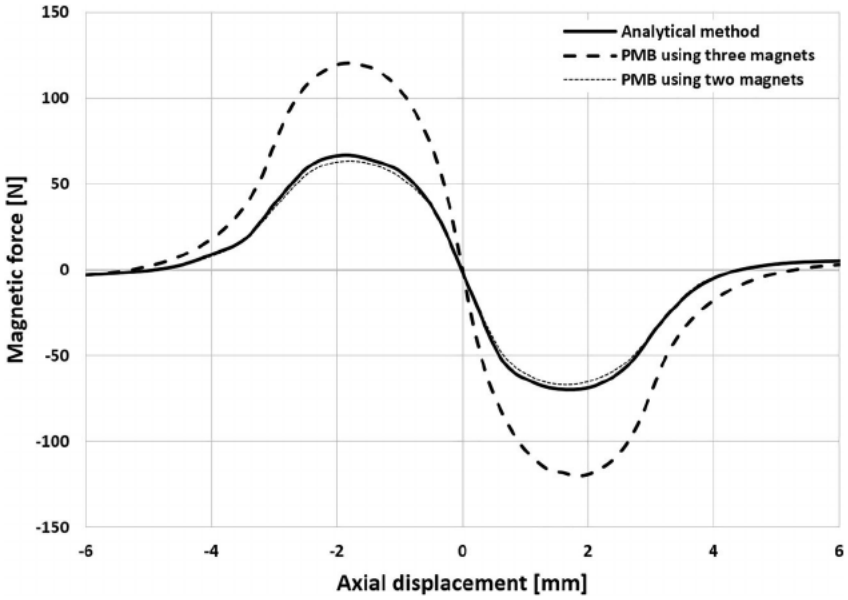

FIGURE 7 Representation of a simple comparison between the magnetic force versus axial displacement in two different structures of PMB and a mechanical ball bearing

Quantity	Value (mm)
Outer radius of the outer ring	31
Inner radius of the outer ring	25
Outer radius of the inner ring	24.9
Inner radius of the inner ring	18.9
Outer ring height	3
Inner ring height	3

Abbreviation: PMB, passive magnetic bearing.

TABLE 2 Dimensions of the tested PMB using two magnetic rings

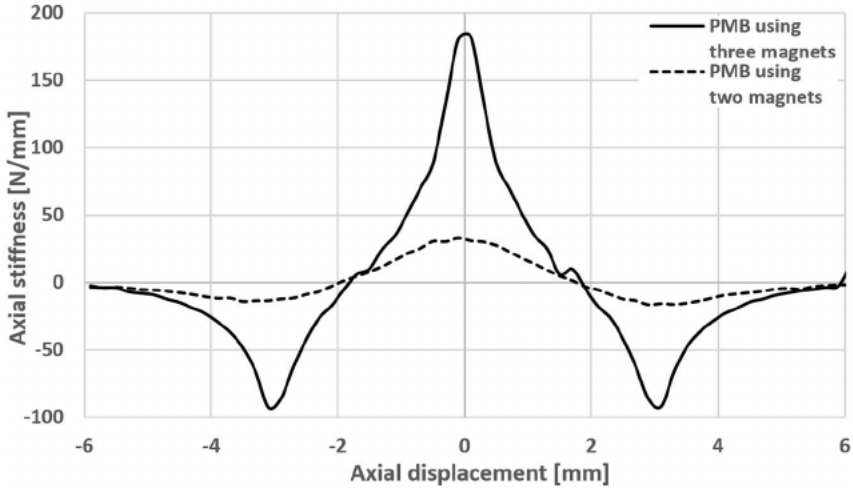

FIGURE 8 Representation of the axial stiffness versus the axial displacement according to the dimensions in Table 1

be the best choice. Also, one of the results of this section is that the force density reaches its maximum amplitude when the three magnets share the same height. So it is utilised in the next section to achieve the optimal height of the magnets as it is shown in Figure 12.

According to Figure 12, the maximum amplitude of the axial force is achieved for a magnets' height between 6 and 7 mm. While the force density is stronger for 5 mm so by considering a trade off between the force amplitude and the force density, 5 mm is selected for the height of three

FIGURE 9 Effect of the air-gap width on the force versus axial displacement of the middle ring PM

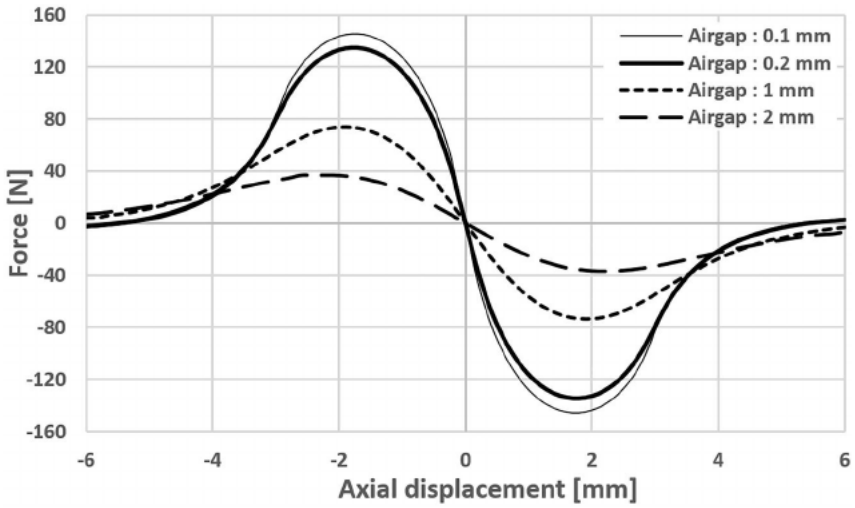

TABLE 3 Dimensions of the proposed PMB for the air-gap width investigation

Symbol	Value (mm)	Symbol	Value (mm)
r_{o_out}	28	r_{m_out} - r_{m_in}	3
r_{o_in}	25	r_{i_out} - r_{i_in}	3
h_o , h_m, h_i	3		

Abbreviation: PMB, passive magnetic bearing.

FIGURE 10 Axial magnetic stiffness versus the axial displacement of the middle ring for different air-gap width

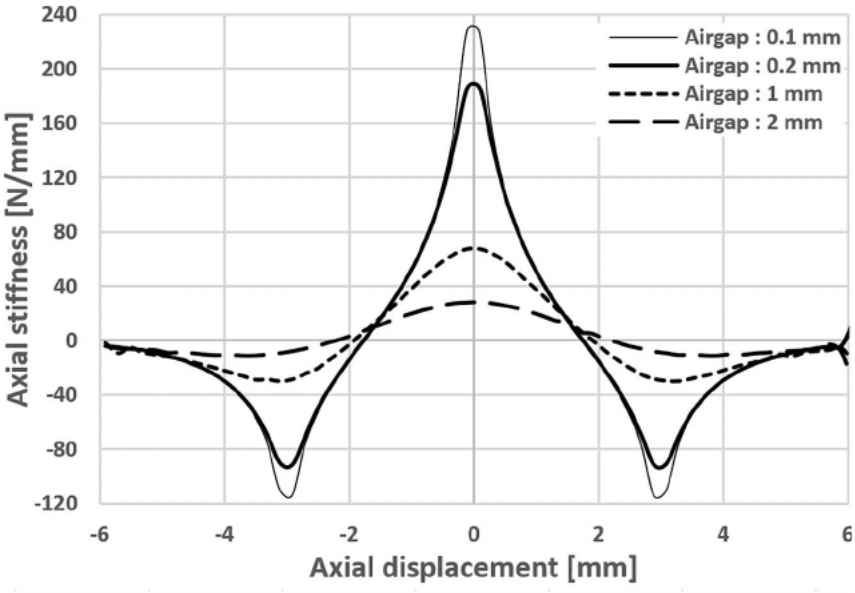

TABLE 4 Dimensions of the proposed PMB for the middle ring height investigation

Symbol	Value (mm)	Symbol	Value (mm)
r_{o_out}	28	r_{i_out}	21.6
r_{o_in}	25	r_{i_in}	18.6
r_{m_out}	24.8	h_o, h_i	3
r_{m_in}	21.8		

Abbreviation: PMB, passive magnetic bearing.

magnets. Then, it will be used in the next sections for all of the rings.

5.3 | Effect of the middle ring width on the force

Table 5 presents the dimensions achieved using the results of the previous steps; while the middle ring width increases, the outer radius of the middle ring is kept constant, as the width of

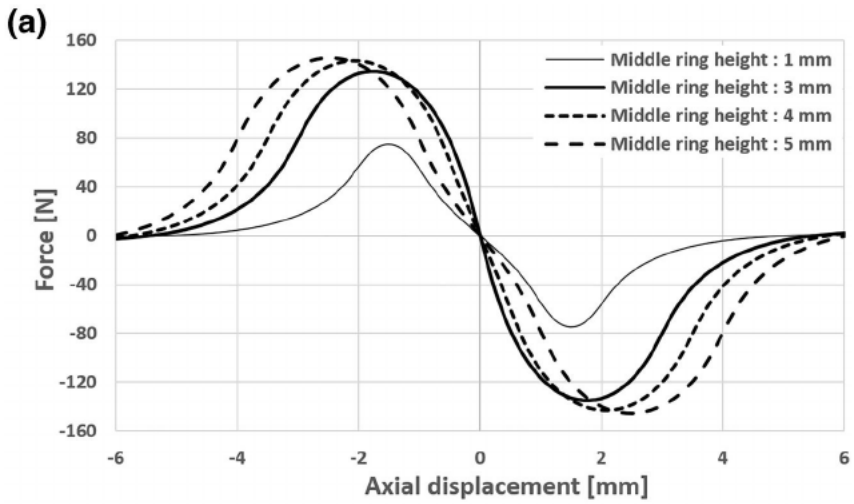

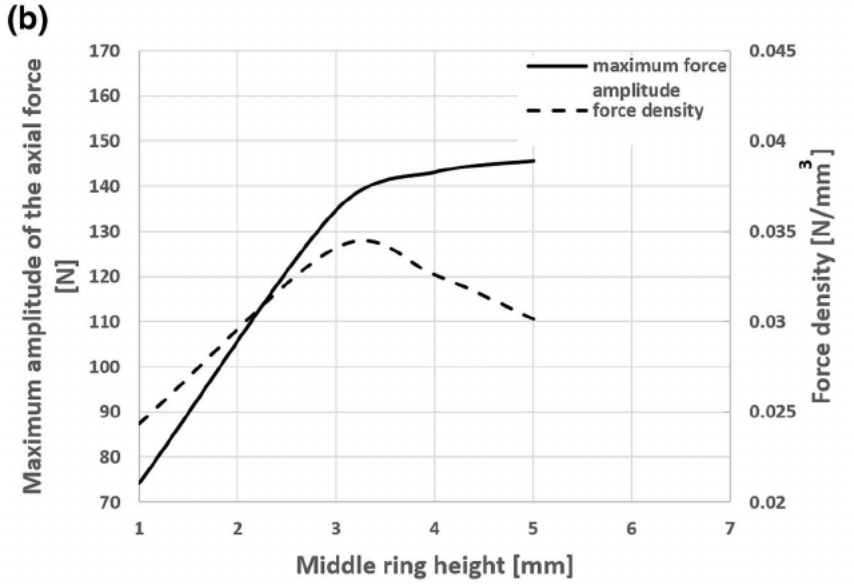

FIGURE 11 Force diagrams: (a) Effect of the middle ring height on the force amplitude versus axial displacement of the middle ring. (b) Trend of the maximum force amplitude together with the force density versus different middle ring heights

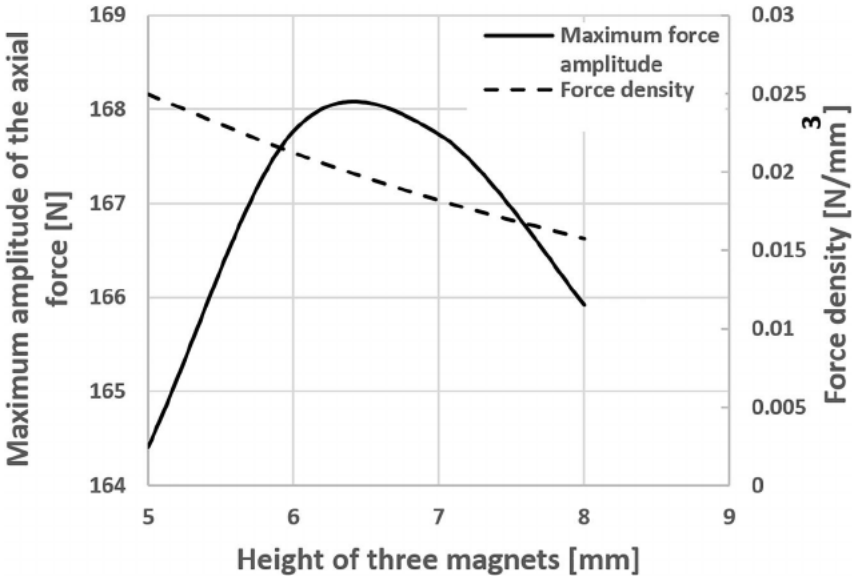

FIGURE 12 Trend of the maximum force amplitude together with the force density versus different heights of three magnets

the inner ring; therefore the inner radius of the inner ring is reduced.

According to Figure 13, the force achieves its maximum amplitude for a middle ring width of 7 mm, while the maximum force density is reachable for the middle ring width of 5 mm. Considering the difference between the maximum force amplitude of 5 and 7 mm, which is 4.67 N, that is 2.41%, and by applying a trade off between the results of these widths, 5 mm was chosen as the better initial middle ring width.

5.4 | Determination of the inner and of the outer rings widths

Inner and outer rings' width is the final parameter that was analysed. To investigate its influence on the force and stiffness, Table 6 presents the best dimensions that were achieved so far. According to Figure 14, the maximum amplitude of the axial force can be achieved when the three PM rings share the same width of 5 mm.

The above results of the sensitivity analysis, which contains the best dimensions of each parameter of PMB, can be helpful to define more effective fitness and penalty functions in GA. Also the initial data are collected from 27 simulations of the PMB aimed at the sensitivity analysis.

6 | OPTIMISATION OF THE NEW STRUCTURE OF PASSIVE MAGNETIC BEARING USING GENETIC ALGORITHM

PMB with two and three PM rings should be optimised to compare. The PMB has some important geometric dimensions which are: air gap, height of rings, width of rings and outer diameter. These dimensions are optimised using the GA. GA exploits the Darwinian theory of the survival of the fittest and utilises an interbreeding population to search the solution of an optimisation problem [30].

The classical GA normally comprises three important operators: selection, crossover and mutation. The air gap length is eliminated from the optimisation as shown in Section 5. The radius of the PMB is added to the optimisation procedure to take into account the volume of the magnets. The definition of the radius in both structures is:

$$r = \frac{r_{o\_out} + r_{i\_in}}{2} \tag{7}$$

The purpose of the objective function is to provide a higher force density in the same displacement. The proposed GA uses the force density as an objective function in order to compare all available structures.

A penalty function was defined to improve the convergence of the optimisation results. In overall, the operation of

TABLE 5 Proposed PMB specification for investigation the middle ring width influence on the force and stiffness

Quantity	Value (mm)	Quantity	Value (mm)
r_{o_out}	28	r_{m_in} - r_{i_out}	0.2
r_{o_in}	25	r_{i_out} - r_{i_in}	3
r_{m_out}	24.8	h_o, h_m, h_i	5

Abbreviation: PMB, passive magnetic bearing.

TABLE 6 Proposed PMB specification for investigation of the inner and of the outer rings widths influence on the force

Quantity	Value (mm)	Quantity	Value (mm)
r_{o_in}	25	r_{i_out}	19.6
r_{m_out}	24.8	h_o, h_m, h_i	5
r_{m_in}	19.8		

Abbreviation: PMB, passive magnetic bearing.

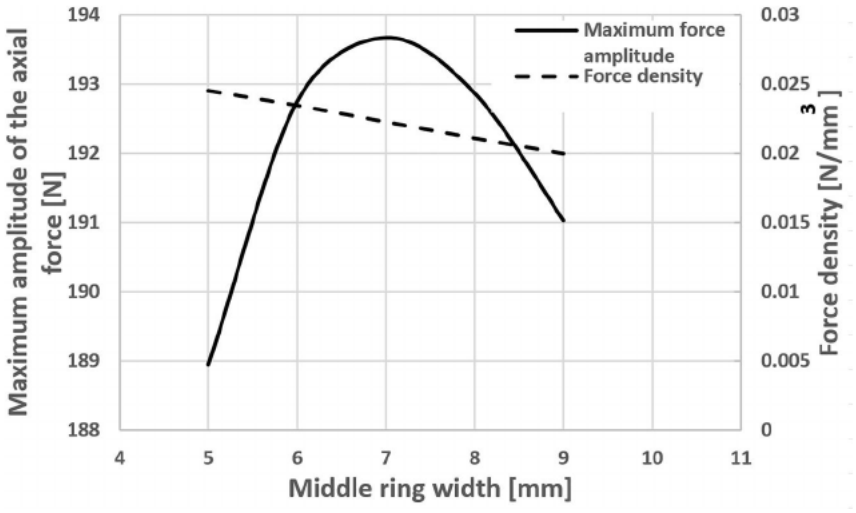

FIGURE 13 Trend of the maximum force amplitude together with the force density versus different middle ring widths

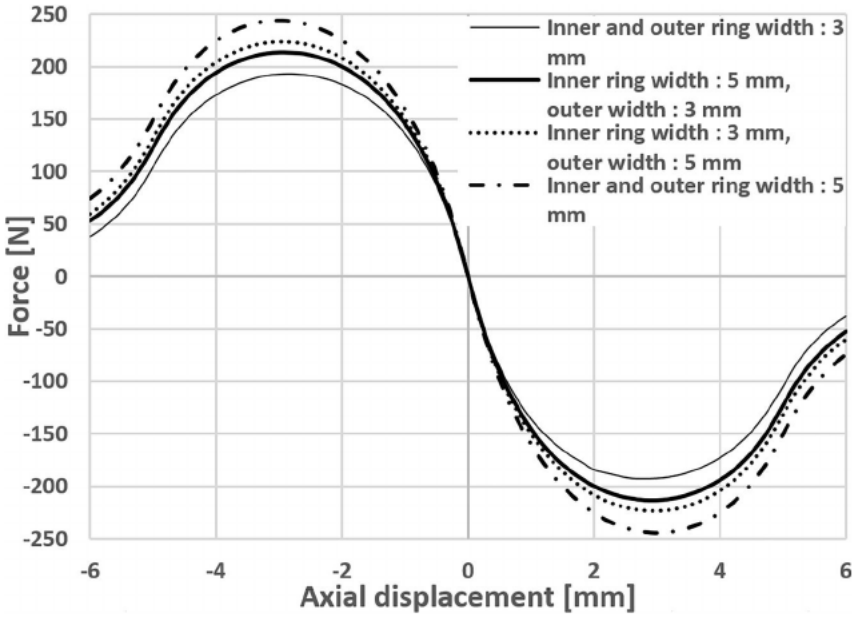

FIGURE 14 Effect of the inner and of the outer rings width on the force

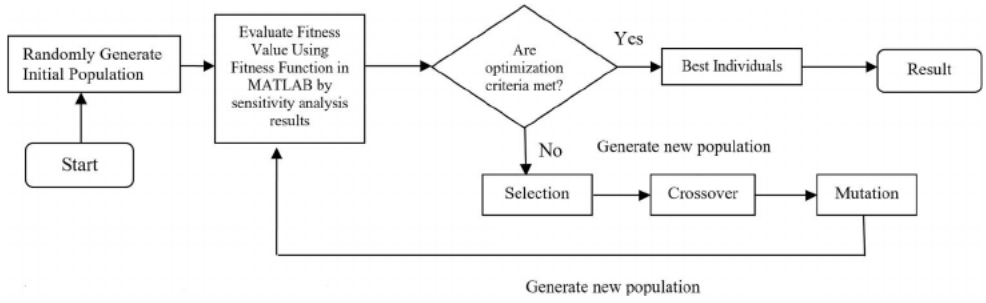

FIGURE 15 Flow chart of the genetic algorithm (GA) in optimizing the passive magnetic bearing (PMB)

GA is classical, and Figure 15 shows the flow chart of GA with its different operators: After accomplishment of sensitivity analysis, acceptable fitness and penalty functions are defined for GA. The results of sensitivity analysis, which was done for each step, will be saved in a database as an initial data for GA. Each member of the population, which is investigated by GA, is introduced as a chromosome including 34 bits in binary format based on the defined dimensions constraints, which are presented in Table 7.

During the GA process, first chromosome is generated randomly, and if this chromosome exists in the database, the needed information such as magnetic force is recalled in order to investigate its force density by objective function; otherwise, the result is produced by interpolation in the database. A new set of variables is generated using genetic operators, and the evolution is addressed towards the best solution according to the objective function. This procedure is continued until the termination criterion is satisfied. A coding including all unknowns is used. The new offspring is added to the best individuals of the old population.

7 | RESULTS AND DISCUSSION

7.1 | Optimisation results

The optimum dimensions of the previous and the proposed structures of PMB are obtained by the maximisation of the force density around the required force amplitude. The results of GA are shown in Table 8. As it is seen, the inner radius of the central magnet is smaller than the inner radius of the corresponding magnet of the two rings PMB. However, the difference is not quite large (less than 1.32 mm), and moreover, the holder of the middle ring can be built to accommodate a larger rotor shaft.

7.2 | Comparison between two structures

Table 9 shows a comparison between the previous and the proposed structures of PMB, according to the optimum dimensions and to their characteristics.

TABLE 7 Optimisation constraints

Dimensional constraints	
Air-gap length (g)	0.2 mm
rings' height (h)	1 mm $\leq h \leq$ 10 mm
rings' width (w)	1 mm $\leq w \leq$ 13 mm
Radius of PMB (r)	20 mm $\leq r \leq$ 30 mm
Defined characteristics	
Magnetic force (F)	190 N $\leq F \leq$ 220 N
Remanent flux density (B_r)	1.15 T

TABLE 8 Design results of PMB using GA

PMB using two PMs		PMB using three PMs	
Item	Gained value (mm)	Item	Gained value (mm)
Height	5.43	Height	3.7
Width	10.4	Width	4.9
Radius	29.92	Radius	25.3
Airgap	0.2	Airgap	0.2
		Middle ring width	4.2

Abbreviation: GA, genetic algorithm; PMs, permanent magnets; PMB, passive magnetic bearing.

TABLE 9 Specification of the PMB for the comparison of the two structures

Item	PMB using two PMs	PMB using three PMs
Magnetic force	208.03 N	204.96 N
Magnetic stiffness	170.0013 N/mm	234.3832 N/mm
Volume of magnets	21233 mm^3	8234 mm^3
Force density	0.0098 N/mm^3	0.0249 N/mm^3

Abbreviation: PM, permanent magnet; PMB, passive magnetic bearing.

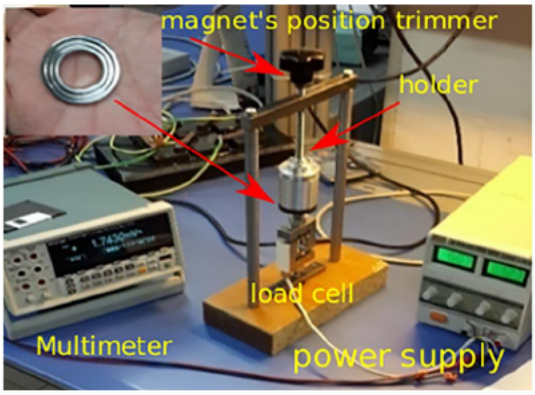

FIGURE 16 Mechanical system for measuring the magnetic force

It can be concluded that both the force density and the magnetic stiffness can be increased significantly in the proposed structure. As it is seen in Figure 2, the complexity of installation is increased in the new structure, but the gained results in the Table 9 shows that the volume of used magnet is decreased significantly, the magnetic stiffness is increased, and also force density is stronger in the new structure; so, the new structure can be considered as a useful PMB in the industry, which provides more advantages than PMB using two magnets.

8 | PRACTICAL RESULTS

To test the validity of the theoretical findings, a test bench is provided, and a practical structure of the proposed PMB with the optimised dimensions was manufactured as shown in Figure 16. As it is seen in Figure 17, two mechanical holders hold the inner and outer rings in their correct position prohibiting radial displacements. This structure is designed to measure magnetic force in different axial displacement of the middle ring inside of the holder; so together with the designed holders, a section is considered in order to exert axial displacement to the middle PM ring, which is connected to the magnet position trimmer, which is a screw connected to the top part of the holder. Actually, by turning the precision screw, the position of the middle ring inside the holder changes. A tension-load-cell S type is attached to the holder to measure the exerted force amplitude due to the displacement. As it is clear, a DC power supply is needed in order to activate the load cell. The voltmeter reading is proportional to the magnetic force between magnets according to the internal constant of the load cell. So in each step, the output of the voltmeter is read, and the related force is calculated.

In order to have more clear investigation, the practical test is applied for measuring the amplitude of magnetic force of PMB using two PMs as shown in Figure 18.

As it can be seen in Figure 19, the maximum amplitude of magnetic force achieved by practical test is 205.05 N, and according to the FEM analysis is 204.2355 N; so, the difference is 0.8145 N, which is 0.39,722%. Also considering Figure 20, the maximum amplitude of the magnetic stiffness achieved by experimental test is 253.6965 N/mm, and based on FEM investigation is 230.323 N/mm, while the difference is 23.3735 N/mm, which is 9.213%. As a consequence of the achieved results, the experimental measurements and FEM results have a good agreement in magnetic force and magnetic stiffness. So, we can conclude that the proposed structure has better characteristics than the classical one, as theoretically predicted.

Also, Figure 20 shows that in the practical structure, the stiffness owns its maximum around the zero displacement, which is conforming with the PMB characteristics, generally.

9 | CONCLUSION

A comparison between two structures of axially magnetised passive magnetic bearings based on finite element analysis has been proposed. The classical two-ring structure was compared

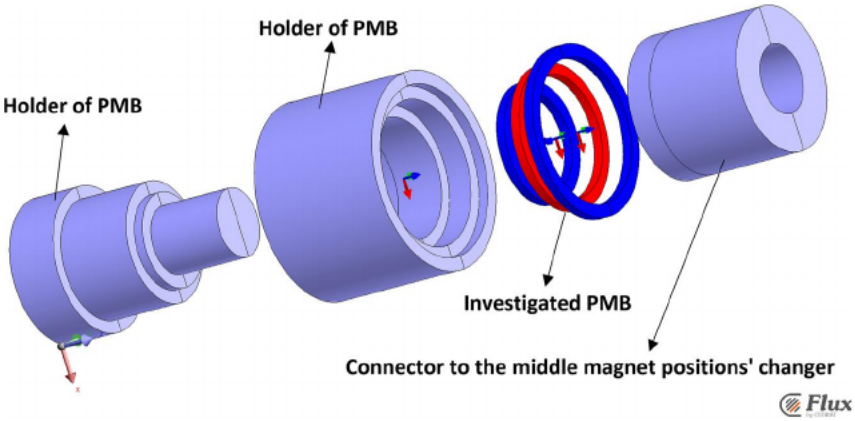

FIGURE 17 Schematic of the designed holder

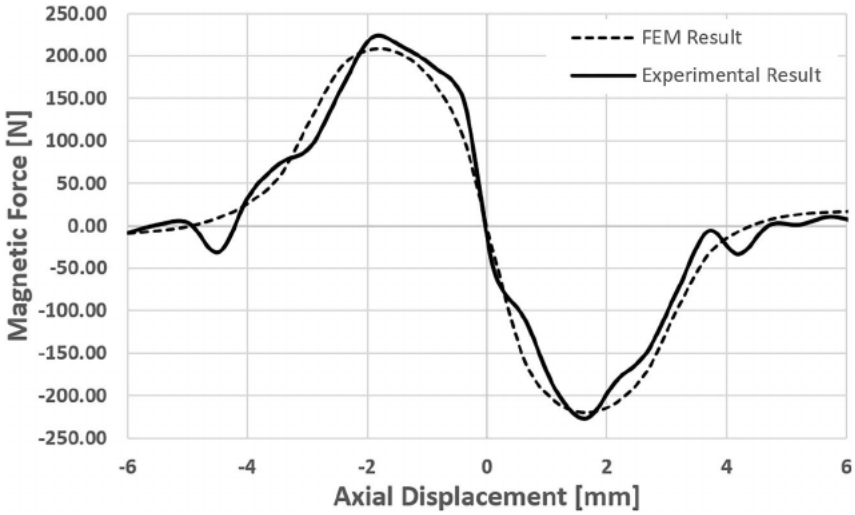

FIGURE 18 Magnetic force versus axial displacement in the practical environment of passive magnetic bearing (PMB) using two permanent magnets (PMs)

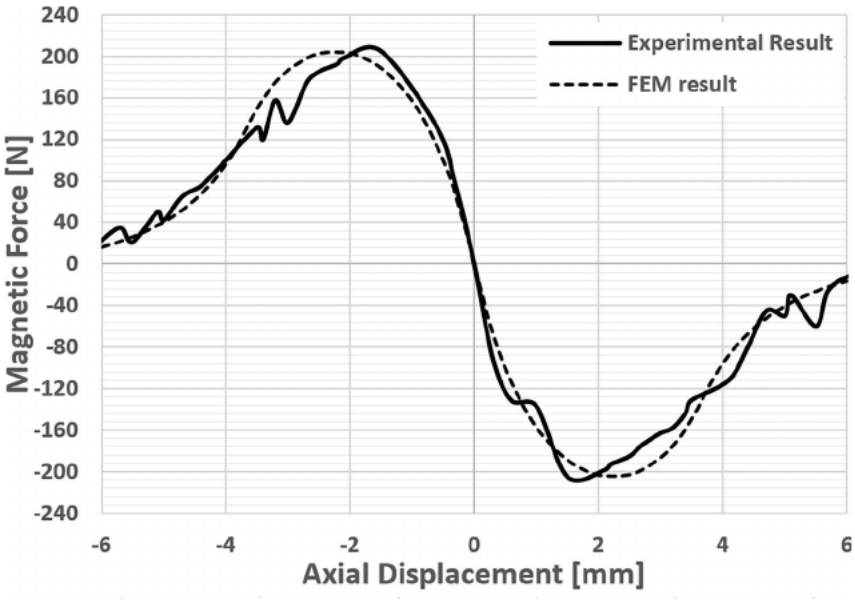

FIGURE 19 Magnetic force versus axial displacement in the practical environment

to the three-ring structure. A new passive magnetic bearing consisting of three ring shape PMs was suggested. A comparison was made between two bearings with optimised dimensions. Sensitivity analysis was done for the new structure using 2D-FEM. Both the axial force and the stiffness are sensitive to changes in the air-gap widths and in the ring

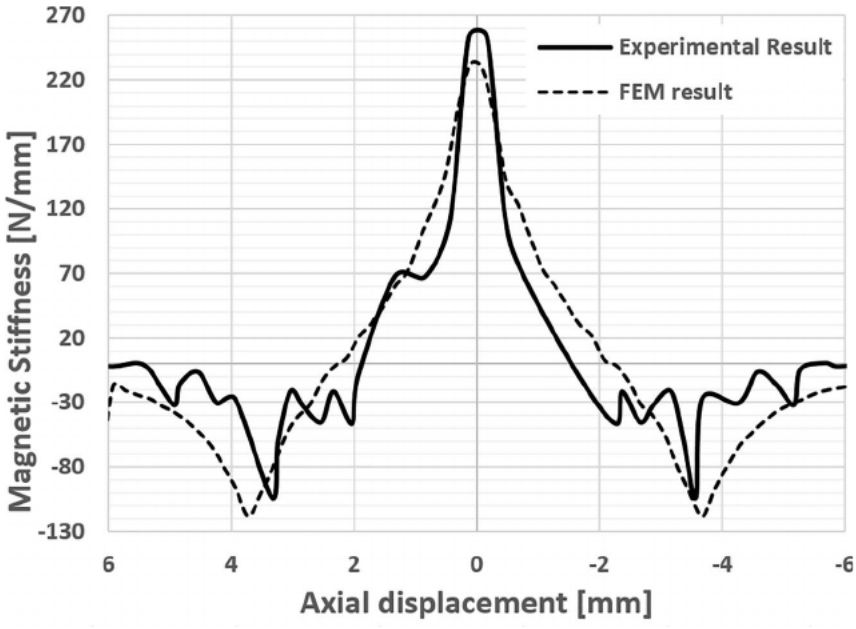

FIGURE 20 Magnetic Stiffness versus axial displacement as the result of the practical test

dimensions. The information gathered in the sensitivity analysis was used to achieve the starting point of a GA, which optimised both structures. The best configurations of both structures producing a given value of the force amplitude with greater force density were determined. FEM simulations were also performed to validate both designs. The new structure provides higher values of stiffness and force density. The bearing is therefore suitable for applications in which high axial force and lighter bearings are required. Future work will include the application of this bearing to pumps for special liquids. In particular, the suitability of the three-ring bearing in supporting the rotor of pumps for artificial heart will be verified. Finally, the study demonstrates that the volume of the active materials of the bearing composed of three rings is lower than that of the classical two-ring passive magnetic bearing.

ORCID

Fabrizio Marignetti https://orcid.org/0000-0001-8776-4561

REFERENCES

1. Cansiz, A., et al.: An effective noncontact torque mechanism and design considerations for an evershed-type superconducting magnetic bearing system. IEEE Trans. Appl. Supercond. 24(1), 22–29 (2014)
2. Marth, E., Jungmayr, G., Amrhein, W.: A 2-d-based analytical method for calculating permanent magnetic ring bearings with arbitrary magnetization and its application to optimal bearing design. IEEE Trans. Magn. 50(5), 1–8 (2014)
3. Mukhopadhyay, S.C., et al.: Design, analysis and control of a new repulsive-type magnetic bearing system. IEEE Proc.-Elec. Power Appl. 146(1), 33–40 (1999)
4. Yanliang, X., et al.: Analysis of hybrid magnetic bearing with a permanent magnet in the rotor by fem. IEEE Trans. Magn. 42(4), 1363–1366 (2006)
5. Eryong, H., Kun, L.: A novel structure for low-loss radial hybrid magnetic bearing. IEEE Trans. Magn. 47(12), 4725–4733 (2011)
6. Eryong, H., Kun, L.: Investigation of axial carrying capacity of radial hybrid magnetic bearing. IEEE Trans. Magn. 48(1), 38–46 (2012)
7. Filatov, A. V., Maslen, E. H.: Passive magnetic bearing for flywheel energy storage systems. IEEE Trans. Magnetics. 37(6), 3913–3924 (2001)
8. Moser, R., Sandtner, J., Bleuler, H.: Optimization of repulsive passive magnetic bearings. IEEE Trans. Magnetics. 42(8), 2038–2042 (2006)
9. Detoni, J.G.: Progress on electrodynamic passive magnetic bearings for rotor levitation. Proc. IME C. J. Mech. Eng. Sci. 228, 1829–1844 (2014)
10. Yonnet, J.P.: Passive magnetic bearings with permanent magnets. IEEE Trans. Magnetics. 14(5), 803–805 (1978)
11. Gotanda, H., Amano, R., Sugiura, T.: Mode coupling of a flexible rotor supported by a superconducting magnetic bearing due to the nonlinearity of electromagnetic force. IEEE Trans. Appl. Supercond. 21(3), 1481–1484 (2011)
12. Fang, J., et al.: Analysis and design of passive magnetic bearing and damping system for high-speed compressor. IEEE Trans. Magn. 48(9), 2528–2537 (2012)
13. Polajzer, B. (ed.).: Magnetic Bearings, Theory and Applications. Sciyo Press, Croatia (2010)
14. Hou, E., Liu, K.: Tilting characteristic of a 2-axis radial hybrid magnetic bearing. IEEE Trans. Magn. 49(8), 4900–4910 (2013)
15. Lee, K.C., et al.: Development of a radial active magnetic bearing for high speed turbo-machinery motors. In: Proceedings of SICE-ICASE International Conference, Busan, Republic of Korea, pp. 1543–1548 (2006)
16. Pichot, M.A., Driga, M.D.: Loss reduction strategies in design of magnetic bearing actuators for vehicle applications. IEEE Trans. Magn. 41(1), 492–496 (2005)
17. Earnshaw, S.: On the nature of the molecular forces, which regulate the constitution of the luminiferous ether. Trans. Cambridge Phil. Soc. 7, 97–112 (1842)
18. Bleuler, H.: A survey of magnetic levitation and magnetic bearing types. JSME Int. J. 35(3), 335–342 (1992)
19. Jiancheng, F., et al.: A new structure for permanent-magnet-biased axial hybrid magnetic bearings. IEEE Trans. Magn. 45(12), 5319–5325 (2009)
20. Jungmayr, G., et al.: Analytical stiffness calculation for permanent magnetic bearings with soft magnetic materials. IEEE Trans. Magnetics. 50(8), 1–8 (2014)
21. Delamare, J., Rulliere, E., Yonnet, J.P.: Classification and synthesis of permanent magnet bearing configurations. IEEE Trans. Magn. 31(6), 4190–4192 (1995)

22. Ravaud, R., et al.: Analytical calculation of the magnetic field created by permanent-magnet rings. IEEE Trans. Magn. 44(8), 1982–1989 (2008)
23. Babic, S., Akyel, C.: Improvement in the analytical calculation of the magnetic field produced by permanent magnet rings. Progr. Electromagn. Res. C. 5, 71–82 (2008)
24. Lijesh, S.B., et al.: Multi-objective optimization of stacked radial passive magnetic bearing. Proc. IME J. J. Eng. Tribol. 232(9), 1140–1159 (2017)
25. Tănase, N., Morega, A. M.: Passive magnetic bearings for flywheel energy storage - numerical design. passive magnetic bearings design. In: Proceedings of International Conference on applied and theoretical electricity (ICATE), Craiova, Romania, pp. 1–4. (October 2014)
26. Lang, M., Lembke, T.A.: Design of permanent magnet bearings with high stiffness. In: Proceedings of 10th International Conference on Magnetic Bearings, Martigny, Switzerland, pp. 221–224 (August 2006)
27. Lang, M., Fremerey, J.K.: Optimization of permanent-magnet bearings. In: Proceedings of 6th International. Conference on Magnetic Suspension Technology, Torino, Italy (2001)
28. Ravaud, R., Lemarquand, G., Lemarquand, V.: Force and stiffness of passive magnetic bearings using permanent magnets. part 1: axial magnetization. IEEE Trans. Magn. 45(7), 2996–3002 (2009)
29. Ravaud, R., Lemarquand, G., Lemarquand, V.: Force and stiffness of passive magnetic bearings using permanent magnets. part 2: radial magnetization. IEEE Trans. Magn. 45(9), 3334–3342 (2009)
30. Alonge, F., et al.: Parameter identification of induction motor model using genetic algorithms. IEE Proc. Contr. Theor. Appl. 145(6), 587–593 (1998)

How to cite this article: Marignetti F, AlizadehTir M, Mirimani SM. An axial passive magnetic bearing using three PM rings. *IET Electr. Power Appl.* 2021;15:415−428. https://doi.org/10.1049/elp2.12030